

# Synthesis and Luminescence Properties of Doped Magnesium Boro-Tellurite Ceramics

Nur Zu Ira Bohari<sup>a,\*</sup>, R. Hussin<sup>a</sup>, Zuhairi Ibrahim<sup>a</sup>, Hendrik O. Lintang<sup>b</sup>

<sup>a</sup>Phosphor Research Group, Department of Physics, Faculty of Science, *Universiti Teknologi Malaysia, 81310 UTM Johor Bahru, Johor Malaysia*

<sup>b</sup>*Ibnu Sina Institute for Fundamental Science Studies, Universiti Teknologi Malaysia, 81310 UTM Johor Bahru, Johor Malaysia*

\*Corresponding author: nzuira@gmail.com

## Article history

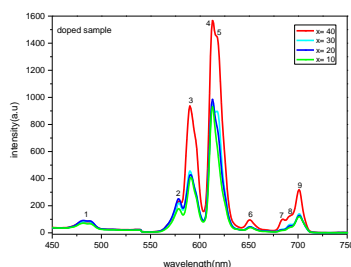
Received: 05 July 2014

Received in revised form:

17 November 2014

Accepted: 1 February 2015

## Graphical abstract



## Abstract

Glass has been widely utilized in the field of lighting, telecommunication and spectroscopy. Boro-tellurite is one of the suitable glasses used for solid state lighting and laser application. The investigation on the luminescence properties of rare earth doped ceramic is rarely used due to the opacity. In this paper boro-tellurite prepared in ceramic can show the better luminescence with the less advantage. The aim of this paper is to present the effect and advantages in luminescence results of boro-tellurite ceramics doped with the constant amount of rare earth. Doped magnesium boro-tellurite with  $\text{Eu}^{3+}$  and  $\text{Dy}^{3+}$  ceramic have been prepared using solid state reaction method with the compositions of  $x\text{TeO}_2-(70-x)\text{B}_2\text{O}_3-30\text{MgO}$  with  $10 \leq x \leq 40$ , and have been doped with  $\text{Eu}_2\text{O}_3$  (1mol%) and  $\text{Dy}_2\text{O}_3$  (1mol%). The characterizations of the samples have been investigated by means of X-Ray diffraction, Raman, Infrared and Photoluminescence spectroscopy. From the X-ray diffraction results, two phases are assigned to  $\text{MgTe}_2\text{O}_5$  and  $\text{Mg}_2\text{B}_2\text{O}_5$ . Raman spectroscopy showed strong bands observed in the vicinity of 140, 175, 220, 266, 332, 403, 436, 646, 694, 723, 757 and  $806 \text{ cm}^{-1}$ . FTIR spectra showed bands located in the range between  $400-800 \text{ cm}^{-1}$  are assigned to the bending mode of Te-O-Te,  $\text{TeO}_3$  and  $\text{TeO}_4$ . In the range of  $800-1400 \text{ cm}^{-1}$ , the bands are associated with B-O, B-O-B,  $\text{BO}_3$  and  $\text{BO}_4$  bonds. The emission transition  $^5\text{D}_0-^7\text{F}_2$  corresponded to the red emission (612 nm) was found to be the most intense in all the  $\text{Eu}^{3+}$ -doped magnesium boro-tellurite ceramics.

**Keywords:** Magnesium boro-tellurite ceramic, luminescence, doped  $\text{Eu}^{3+}$  and  $\text{Dy}^{3+}$

## Abstrak

Kaca telah digunakan secara meluas dalam bidang pencahayaan, telekomunikasi dan spektroskopi. Boro-tellurite adalah satu kaca yang sesuai digunakan dalam pencahayaan keadaan pepejal dan aplikasi laser. Penyelidikan luminesens bagi nadir bumi dop seramik adalah jarang digunakan disebabkan oleh kelegapan. Dalam kertas ini boro-tellurite seramik menunjukkan luminesens yang baik dengan kelebihan kurang. Matlamat kertas ini adalah untuk menunjukkan kesan dan kelebihan dalam keputusan luminesens bagi seramik boro-tellurite dop dengan amoun nadir bumi yang tetap. Dop magnesium boro-tellurite dengan  $\text{Eu}^{3+}$  and  $\text{Dy}^{3+}$  seramik disediakan dengan menggunakan kaedah tindakbalas keadaan pepejal yang berkompposisi  $x\text{TeO}_2-(70-x)\text{B}_2\text{O}_3-30\text{MgO}$  dengan  $10 \leq x \leq 40$ , dan dop  $\text{Eu}_2\text{O}_3$  (1mol%) and  $\text{Dy}_2\text{O}_3$  (1mol%). Pencirian sampel disiasat oleh spektroskopi pembelauan sinar-X, Raman, infra merah and Fotoluminesens. Dari keputusan XRD, dua fasa dilihat sebagai  $\text{MgTe}_2\text{O}_5$  and  $\text{Mg}_2\text{B}_2\text{O}_5$ . Spektroskopi Raman menunjukkan jalur kuat dilihat sekitar 140, 175, 220, 266, 332, 403, 436, 646, 694, 723, 757 dan  $806 \text{ cm}^{-1}$ . Spektra FTIR menunjukkan jalur terletak dalam lingkungan  $400-800 \text{ cm}^{-1}$  adalah mod lentur bagi Te-O-Te,  $\text{TeO}_3$  and  $\text{TeO}_4$ . Dalam lingkungan  $800-1400 \text{ cm}^{-1}$ , jalur yang berkaitan adalah B-O, B-O-B,  $\text{BO}_3$  and  $\text{BO}_4$ . Peralihan pancaran  $^5\text{D}_0-^7\text{F}_2$  yang merujuk kepada pancaran merah (612 nm) didapati menjadi yang paling tinggi dalam semua seramik  $\text{Eu}^{3+}$ -dop magnesium boro-tellurite.

**Kata kunci:** Seramik magnesium boro-tellurite, luminesens, dop  $\text{Eu}^{3+}$  and  $\text{Dy}^{3+}$

© 2015 Penerbit UTM Press. All rights reserved.

## 1.0 INTRODUCTION

Ceramic based on boro-tellurite host matrices doped with rare earth have tremendous applications for lasers, optical amplifier, photo sensitivity, optical storage, and bio-ceramics materials [1-8]. Currently, a great deal of research has been focused on rare earth

(RE) doped glasses owing to their extensive applications [9-10]. But, the investigation on the luminescence properties of rare earth doped ceramic is rarely used due to the opacity and hence, limited their applications.  $\text{Eu}^{3+}$  ion doped sodium-aluminum-tellurite ( $\text{Eu}^{3+}$ : NAT) was prepared in opaque ceramics compound [11].

The host material with low phonon energy that can reduce the non-radiative loss, play important role for obtaining highly efficient luminescent properties via multiphonon relaxations and thus achieve strong luminescence [12]. In this study, tellurite oxide based has been utilized due to their desirable physical properties, such as high refractive index, excellent infrared transmittance and high dielectric constant, good chemical durability and low melting temperature. On the other hand, borate has important physical properties such as high transparency, low melting point, high thermal stability, good rare earth ions solubility, resistance to

## 2.0 EXPERIMENTAL

High purity of  $\text{H}_3\text{BO}_3$  (99.99%),  $\text{TeO}_2$  (99.99%),  $\text{MgO}$  (99.99%),  $\text{Eu}_2\text{O}_3$  (99.99%) and  $\text{Dy}_2\text{O}_3$  (99.99%) were used as the raw materials. Two types of sample were prepared for the study; magnesium boro-tellurite ceramic and magnesium boro-tellurite with  $\text{Eu}^{3+}$  and  $\text{Dy}^{3+}$  ceramic. The samples with the compositions of  $x\text{TeO}_2-(70-x)\text{B}_2\text{O}_3-30\text{MgO}$  with  $10 \leq x \leq 40$  mol%, doped with  $\text{Eu}_2\text{O}_3$  (1mol%) and  $\text{Dy}_2\text{O}_3$  (1mol%) have been prepared using solid state reaction method. Analytical grade reagents of  $\text{H}_3\text{BO}_3$ ,  $\text{TeO}_2$ ,  $\text{MgO}$ ,  $\text{Eu}_2\text{O}_3$  and  $\text{Dy}_2\text{O}_3$  powders in appropriate amounts (mol%) were thoroughly mixed in agate mortar. The mixtures were pressed into pellets using hydraulic press with  $10 \text{ ton/cm}^2$  of pressure. Pelletized samples were then heat treated at  $650 \text{ }^\circ\text{C}$  for 6 hours. The dried pellet was grounded into fine powder for further characterizations.

Several experiments have been setup to determine the physical nature and characteristics of the prepared samples. The examination of the structure was examined using X-ray diffraction (XRD) using Siemens Diffraction D500 diffractometer with  $\text{CuK}\alpha$  radiation [13]. Fourier transform infrared spectroscopy (FTIR) was examined using Perkin-Elmer spectrometer (Spectrum 100) [13]. Raman spectroscopy was examined using Bruker model RFS 100/S FT-Raman spectrometer. The emission spectra were obtained using Jasco Fluorescence spectrophotometer, Model FP8000 series, at room temperature.

## 3.0 RESULTS AND DISCUSSION

X-ray diffraction technique was used to identify the crystalline phase of the doped magnesium boro-tellurite with  $\text{Eu}^{3+}$  and  $\text{Dy}^{3+}$  ceramics. The XRD patterns, Figure 1, show the influence of varying composition of the  $x\text{TeO}_2-(70-x)\text{B}_2\text{O}_3-30\text{MgO}$  with  $10 \leq x \leq 40$  mol%. The x-ray diffractogram showed well-defined peaks which indicate the crystalline and phase formation of the synthesized compounds. There are two main phases; namely  $\text{MgTe}_2\text{O}_5$  (ICDD: 01-073-3922) and  $\text{Mg}_2\text{B}_2\text{O}_5$  (ICDD: 01-073-2107). The intensity increased with  $\text{B}_2\text{O}_3$  and decrease with  $\text{TeO}_2$ , ranging from  $x = 10$  to 40.  $\text{MgTe}_2\text{O}_5$  became a dominant phase in the sample followed by  $\text{Mg}_2\text{B}_2\text{O}_5$  phase. The majority phase of  $\text{MgTe}_2\text{O}_5$  is an evident that the  $\text{TeO}_2$  contribute to the formation of the phase. The percentage of the crystalline phase can be estimated by comparing the highest peak heights summarized in the Table 1. From the estimation of Table 1, it can be concluded that the  $\text{MgTe}_2\text{O}_5$  was the dominant phase.

chemicals and can enhance mechanical durability [3]. Addition of alkali oxide ( $\text{MgO}$ ) as network modifier has also been employed since the utilization of modifier doped with boro-tellurite based are rarely reported.

The aim of this work is to prepare doped magnesium boro-tellurite ceramics via solid state reaction route and to study the behavior through X-Ray Diffraction (XRD), Infrared (IR), Raman and Photoluminescence (PL) spectroscopic for both materials. The concentration of  $\text{Eu}^{3+}$  and  $\text{Dy}^{3+}$  will remain constant.

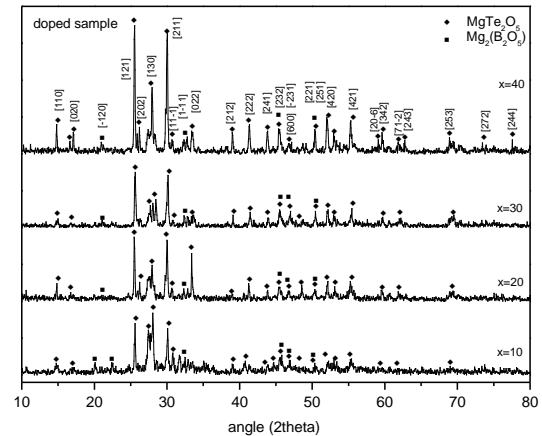


**Figure 1** X-ray diffraction pattern of  $x\text{TeO}_2-(70-x)\text{B}_2\text{O}_3-30\text{MgO}$  doped  $\text{Eu}^{3+}$  and  $\text{Dy}^{3+}$  ceramic ( $10 \leq x \leq 40$  mol%)

**Table 1** The estimation of percentage of the crystalline phase of  $x\text{TeO}_2-(70-x)\text{B}_2\text{O}_3-30\text{MgO}$  doped  $\text{Eu}^{3+}$  and  $\text{Dy}^{3+}$  ceramic ( $10 \leq x \leq 40$  mol%)

$x$	$\text{MgTe}_2\text{O}_5$ phase (%)	$\text{Mg}_2\text{B}_2\text{O}_5$ phase (%)
10	58.03	41.97
20	62.94	37.05
30	67.94	32.06
40	76.00	23.99

Raman spectrum of  $x\text{TeO}_2-(70-x)\text{B}_2\text{O}_3-30\text{MgO}$  are presented in Figure 2. Raman spectroscopy show the strong band are observed at 140, 175, 220, 266, 332, 403, 436, 646, 694, 723, 757 and  $806 \text{ cm}^{-1}$ . Raman spectrum shows that besides the expected  $\text{TeO}_4$ ,  $\text{TeO-Te}$ , and  $\text{BO}_3$  (peak 7 to 12) existent, the vibrations corresponding to the metal ions are also present in ceramics (peak 1 to 6), respectively.

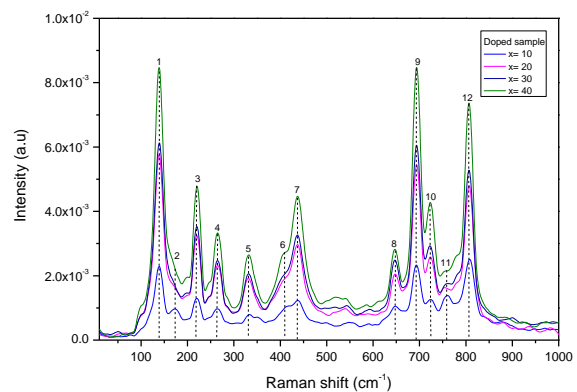


**Figure 2** Raman spectra of  $x\text{TeO}_2-(70-x)\text{B}_2\text{O}_3-30\text{MgO}$  doped  $\text{Eu}^{3+}$  and  $\text{Dy}^{3+}$  ceramic ( $10 \leq x \leq 40$  mol%)

The infrared spectrum of  $x\text{TeO}_2-(70-x)\text{B}_2\text{O}_3-30\text{MgO}$  with  $10 \leq x \leq 40$  mol% in the range  $1400-4000\text{cm}^{-1}$  are presented in the Figure 3. There are four bands in this range in which the peaks represent OH- and H- units are at around  $3215\text{cm}^{-1}$ ,  $2920\text{cm}^{-1}$  and  $2261\text{cm}^{-1}$ . The peaks observed between  $3375\text{cm}^{-1}$  and  $4000\text{cm}^{-1}$  are the hydroxyl groups due to OH- stretching and the peaks observed between  $(2800-2900)\text{cm}^{-1}$  are the hydrogen bond [9]. Based on the Figure 3, the peaks around  $1500\text{cm}^{-1}$  are due to the B-O stretching of  $\text{BO}_3$  units which are observed and the band became smaller ( $x=40$ ), indicating a decrease in  $\text{TeO}_2$  amounts and increasing  $\text{B}_2\text{O}_3$ .

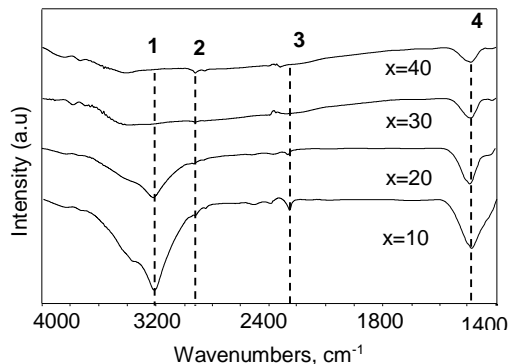


**Figure 3** IR spectra of  $x\text{TeO}_2-(70-x)\text{B}_2\text{O}_3-30\text{MgO}$  doped  $\text{Eu}^{3+}$  and  $\text{Dy}^{3+}$  ceramic ( $10 \leq x \leq 40$  mol%)

In Figure 4, the IR spectra of  $x\text{TeO}_2-(70-x)\text{B}_2\text{O}_3-30\text{MgO}$  with  $10 \leq x \leq 40$  mol% in the range  $(800-1400)\text{cm}^{-1}$  is presented. The bands located in the range between  $(400-800)\text{cm}^{-1}$  are assigned to the bending mode of  $\text{Te-O-Te}$ ,  $\text{TeO}_3$  and  $\text{TeO}_4$ . In the range of  $(800-1400)\text{cm}^{-1}$ , the B-O bond of  $\text{B-O-B}$ ,  $\text{BO}_3$  and  $\text{BO}_4$  also appeared. The bands located around  $(1331-1362)\text{cm}^{-1}$  are assigned to  $\text{BO}_3$  units [15, 21] and in the range between  $(881-1200)\text{cm}^{-1}$  which is the  $\text{BO}_4$  units [10, 14, 16]. The bands positions around  $431\text{cm}^{-1}$ ,  $564\text{cm}^{-1}$ ,  $610-680\text{cm}^{-1}$  and  $700-780\text{cm}^{-1}$  showed the  $\text{Te-O-Te}$ ,  $\text{TeO}_2$  and  $\text{TeO}_3$  respectively. All of these assignments are in good agreement with the reported literature [10, 17-18]. In Figure 4, the band gradually increased with  $\text{TeO}_2$ . The intensity of the band in the range of  $431-780\text{cm}^{-1}$  increased gradually with  $\text{TeO}_2$  and the intensity of the band slightly decreased with  $\text{B}_2\text{O}_3$  in the range of  $881-1362\text{cm}^{-1}$ .

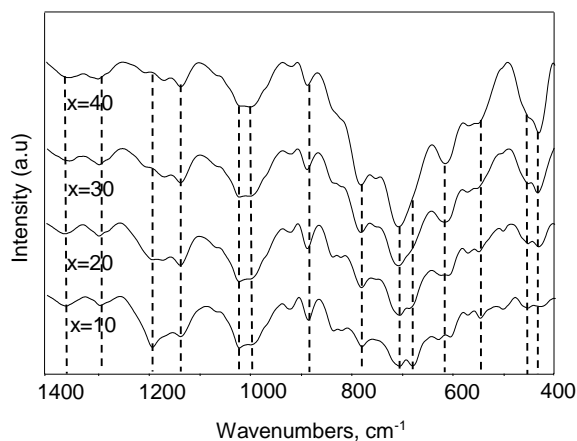


**Figure 4** IR spectra of  $x\text{TeO}_2-(70-x)\text{B}_2\text{O}_3-30\text{MgO}$  doped  $\text{Eu}^{3+}$  and  $\text{Dy}^{3+}$  ceramic ( $10 \leq x \leq 40$  mol%)

The emission spectrum of doped  $x\text{TeO}_2-(70-x)\text{B}_2\text{O}_3-30\text{MgO}$  with  $10 \leq x \leq 40$  mol% is shown in Figure 5. The emission transitions

$^5\text{D}_0 \rightarrow ^7\text{F}_0$ ,  $^5\text{D}_0 \rightarrow ^7\text{F}_0$ ,  $^5\text{D}_0 \rightarrow ^7\text{F}_1$ ,  $^5\text{D}_0 \rightarrow ^7\text{F}_2$ ,  $^5\text{D}_0 \rightarrow ^7\text{F}_2$ ,  $^5\text{D}_0 \rightarrow ^7\text{F}_3$ ,  $^5\text{D}_0 \rightarrow ^7\text{F}_4$ ,  $^5\text{D}_0 \rightarrow ^7\text{F}_4$  and  $^5\text{D}_0 \rightarrow ^7\text{F}_4$  corresponded to the band position at  $484.58$ ,  $578.17$ ,  $589.89$ ,  $612.82$ ,  $618.38$ ,  $651.23$ ,  $683.48$ ,  $691.53$  and  $700.85\text{nm}$ , respectively. It can be noted that a series of  $\text{Eu}^{3+}$  characteristic emission lines are between  $540\text{nm}$  and  $780\text{nm}$ , which includes the most prominent peak at  $612\text{nm}$  and corresponding to the  $^5\text{D}_0 \rightarrow ^7\text{F}_J$  ( $J=0, 1, 2, 3, 4$ ) transitions [19]. The luminescence spectrum was found to be lowest for the sample  $x=10$  followed by  $x=20, 30$  and  $40$ . The  $^5\text{D}_0 \rightarrow ^7\text{F}_2$  transition is more intense than the other transitions as reported in the other literatures [20-22].

The emission peaks of  $\text{Dy}^{3+}$  were observed at  $484.58\text{nm}$  and  $578.17\text{nm}$  (peak 1 and 2) similar with the other reported values [23]. Figure 5 shows the emission peaks of  $\text{Eu}^{3+}$  are more dominant with high intensity compared the peaks of  $\text{Dy}^{3+}$ . The  $\text{Dy}^{3+}$  emission peaks are not present as dominant peak which indicates that  $\text{Dy}^{3+}$  acts as trap centers that cause long afterglow characteristics, rather than the luminescent centers in the host lattice [24].

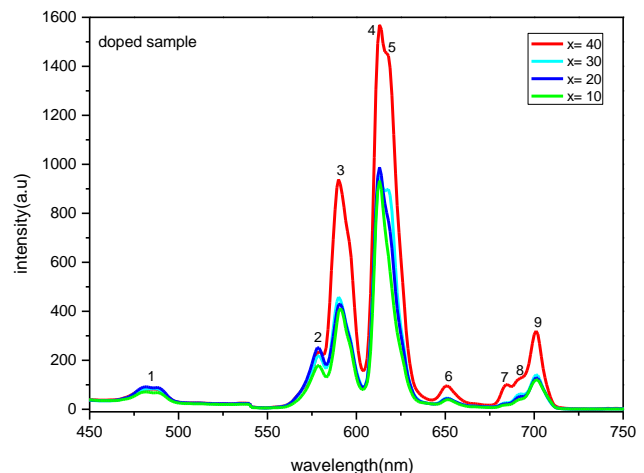


**Figure 5** Emission spectrum of  $x\text{TeO}_2-(70-x)\text{B}_2\text{O}_3-30\text{MgO}$  doped  $\text{Eu}^{3+}$  and  $\text{Dy}^{3+}$  ceramic ( $10 \leq x \leq 40$  mol%)

#### 4.0 CONCLUSION

The samples of  $x\text{TeO}_2-(70-x)\text{B}_2\text{O}_3-30\text{MgO}$  with  $10 \leq x \leq 40$  mol% doped with  $\text{Eu}_2\text{O}_3$  (1 mol%) and  $\text{Dy}_2\text{O}_3$  (1 mol%) have been prepared using solid state route. The structural studies of the samples have been investigated using X-ray diffraction (XRD), Infrared and Raman spectroscopy. The XRD profiles show that  $\text{MgTe}_2\text{O}_5$  became a dominant phase in the sample followed by  $\text{Mg}_2\text{B}_2\text{O}_5$  phase. The IR spectrum shows two series of band regions which obtained in  $4000-1400\text{cm}^{-1}$  and the second region of  $1400-400\text{cm}^{-1}$ . The ceramics doped with  $\text{Eu}^{3+}$  shows a bright red emission at  $612\text{nm}$  which belongs to the electric dipole ( $^5\text{D}_0 \rightarrow ^7\text{F}_2$ ) transition of  $\text{Eu}^{3+}$  ions. There are two groups of emission at  $484\text{nm}$  and  $578\text{nm}$  occurring in the emission spectrum of the ceramics, which probably can be applied for white LEDs application.

#### Acknowledgement

The authors would like to acknowledge the financial supports from the Fundamental Research Grant Scheme (FRGS) under research grant Project Number: R.J130000.7826.4F140 and the authors would like to thanks Faculty of Science, Universiti Teknologi Malaysia for providing the facilities.

## References

- [1] Mallawany, R. 1992. The Optical Properties of Tellurite Glasses. *Journal of Appl. Phys.* 72: 1774.
- [2] Babu, P., H.J. Seo, K.H. Jang, K.U. Kumar, C.K. Jayasankar. 2007. Optical Spectroscopy, 1.5 $\mu$ m Emission, and Upconversion Properties of Er<sup>3+</sup>-doped Metaphosphate Laser Glasses. *Chem. Phys. Letter* 445: 162.
- [3] Joshi, P., S. Shen, and A. Jha. 2008. Er<sup>3+</sup>-doped Boro-Tellurite Glass for Optical Amplification in the 1530-1580 nm. *Journal of Appl. Phys.* 103: 083543.
- [4] Sudhakar, B. and S. Buddhudu. 2008. Spectral Analysis of Nd<sup>3+</sup> & Er<sup>3+</sup>:B<sub>2</sub>O<sub>3</sub>-(TeO<sub>2</sub>/CdO/ZnO)-Li<sub>2</sub>O-AlF<sub>3</sub> glasses. *Journal of Optoelectron. Adv. Mater.* 10: 2777–2781.
- [5] Rada, S., E. Culea, V. Rus, M. Pica and M. Culea. 2008. The Local Structure of Gadolinium Vanado-Tellurite Glasses. *Journal of Materials Science*. 43: 3713–3716.
- [6] Konijnendijk, W.L. and J.M. Stevels. 1975. The Structure of Borate Glass Studied by Raman Scattering. *Journal of Non-Cryst. Solids*. 18: 30.
- [7] Bhargava, A.,R.L. Snyder and R.A. Condrate. 1987. The Raman and IR spectroscopy of the Glasses in the System of BaO.TiO<sub>2</sub>.B<sub>2</sub>O<sub>3</sub>. *Mater. Res. Bull.* 22: 1603.
- [8] Pascuta, P., L. Pop, S. Rada, M. Bosca, and E. Culea. 2008. The Local Structure of Bismuth Borate Glasses doped with Europium Ions Evidenced by FT-IR Spectroscopy. *Journal of Materials Science Materials in Electronics*. 19: 424–428.
- [9] Maheshvaran, K. and K. Marimuthu. 2011. Structural and Optical Investigations on Dy<sup>3+</sup> doped Boro-Tellurite Glasses. *Journal of Alloys and Compounds*. 509: 7427–7433.
- [10] Selvaraju, K., K. Marimuthu, T.K. Seshagiri, S.V. Godbole. 2011. Thermal, Structural and Spectroscopic Investigations on Eu<sup>3+</sup> doped Boro-Tellurite Glasses. *Journal of Materials Chemistry and Physics* 131: 204–210.
- [11] Chen, B.J., E.Y.B. Pun, H. Lin. 2009. Photoluminescence and Spectral Parameters Eu<sup>3+</sup> in Sodium-Aluminum-Tellurite Ceramics. *Journal of Alloys and Compounds*. 479: 352–356.
- [12] Alias, N.S., R. Hussin, M.A. Salim, S.A.A. Fuzi, M. S. Abdullah, S. Abdullah and M. N. M. Yusof. 2009. Structural Studies on Magnesium Calcium Tellurite doped with Eu<sup>2+</sup> and Dy<sup>3+</sup>. *Solid State Science and Technology*. 17:50–58.
- [13] Bohari, N.Z.I, R. Hussin, Z. Ibrahim, M.H. Haji Jumali, R. Uning and A. Rohaizad. 2014. Structural and luminescence properties of Eu<sup>3+</sup> and Dy<sup>3+</sup>-doped Magnesium Boro-Tellurite ceramics. *Advanced Materials Research*. 895: 269–273.
- [14] Dwivedi, B.P. and B.N. Khanna. 1995. Cation Dependence of Raman Scattering in Alkali Borate Glasses. *J. Phys. Chem. Solids*. 1: 39–49.
- [15] Pavani, P.G., S. Suresh and V.C. Mouli. 2011. Studies on Boro Cadmium Tellurite Glasses, *J. of Optical Materials* 34: 215–220.
- [16] Maheshvaran, K., K. Linganna and K. Marimuthu. 2011. Composition Dependent Structural and Optical Properties of Sm<sup>3+</sup> doped Boro-Tellurite Glasses. *Journal of Luminescence*. 131: 2746–2753.
- [17] Rada, S., M. Culea and E. Culea. 2008. Structure of TeO<sub>2</sub>.B<sub>2</sub>O<sub>3</sub> Glasses Inferred from Infrared Spectroscopy and DFT Calculations. *Journal of Non-Crystalline Solid*. 354: 5491–5495.
- [18] Azevedo, J., J. Coelho, G. Hungerford and N.S. Hussain. 2010. Lasing Transition (<sup>4</sup>F<sub>3/2</sub>→<sup>4</sup>I<sub>11/2</sub>) at 1.06 $\mu$ m in Neodymium Oxide doped Lithium Boro Tellurite Glass. *J. of Physica B*. 405: 4696–4701.
- [19] Lourenco, S.A., N.O. Dantas, E.O. Serqueira, W.E.F. Ayta, A.A. Andrade, M.C. Filadelpho, J.A. Sampaio, M.J.V. Bell and M.A. Pereira. 2011. Eu<sup>3+</sup> Photoluminescence Enhancement due to the Thermal Energy Transfer in Eu<sub>2</sub>O<sub>3</sub>-doped SiO<sub>2</sub>-B<sub>2</sub>O<sub>3</sub>-PbO<sub>2</sub> Glasses System. *Journal of Luminescence*. 131: 850–855.
- [20] Lavin, V., P. Babu, C.K. Jayasankar, I.R. Martin and V.D. Rodriguez. 2001. On the Local Structure of Eu<sup>3+</sup> ions in OxyfluorideGlasses. Comparison with Fluoride and Oxide Glasses. *J. of Chemical Physics*. 115: 10935–10944.
- [21] Venkatramu, V., P. Babu and C.K. Jayasankar. 2006. Fluorescence properties of Eu<sup>3+</sup>ions doped Borate and Fluoroborate Glasses Containing Lithium, Zinc and Lead, *Spectrochimica Acta Part A*. 63: 276–281.
- [22] Venkatramu, V., D. Navarro, P. Babu, C.K. Jayasankar, V. Lavin. 2005. Fluorescence Line Narrowing spectral studies of Eu<sup>3+</sup>-doped Lead Borate Glass. *J. Non-Cryst. Solids*. 351: 929.
- [23] Lakshminarayana, G. and J. Qiu. 2008. Photoluminescence of Pr<sup>3+</sup>, Sm<sup>3+</sup> and Dy<sup>3+</sup>:SiO<sub>2</sub>-Al<sub>2</sub>O<sub>3</sub>-LiF-GdF<sub>3</sub> glass Ceramics and Sm<sup>3+</sup>, Dy<sup>3+</sup>: GeO<sub>2</sub>-B<sub>2</sub>O<sub>3</sub>-ZnO-LaF<sub>3</sub> Glasses. *Physica B*. 404: 1169–1180.
- [24] Lin, Y., Z. Zhang, Z. Tang, X. Wang, J. Zhang and Z. Zheng. 2001. Luminescent Properties of a New Long Afterglow Eu<sup>3+</sup> and Dy<sup>3+</sup> Activated Ca<sub>3</sub>MgSi<sub>2</sub>O<sub>8</sub> Phosphor. *Journal of the European Ceramic Society*. 21: 683–685.